sustainability

Article

Enhancing the Durability Properties of Sustainable Geopolymer Concrete Using Recycled Coarse Aggregate and Ultrafine Slag at Ambient Curing

Saloni Arora [1], Parveen Jangra [2,*], Thong M. Pham [3,*] and Yee Yan Lim [1]

1 Faculty of Science & Engineering, Southern Cross University, Lismore, NSW 2477, Australia
2 Department of Civil Engineering, Deenbandhu Chhotu Ram University of Science and Technology, Murthal 131039, Haryana, India
3 Center for Infrastructural Monitoring and Protection, School of Civil and Mechanical Engineering, Curtin University, Kent Street, Bentley, WA 6102, Australia
* Correspondence: separveenjangra@dcrustm.org (P.J.); thong.pham@curtin.edu.au (T.M.P.)

Abstract: This study aimed at investigating the durability characteristics of the ambient-cured geopolymer concrete (GPC) developed using recycled coarse aggregate (RCA) and ultrafine slag (UFS). Two series of mixes were prepared. Natural aggregates (NAs) were replaced by RCA at different volume levels of 0, 25, 50 and 100% in both series. Meanwhile, UFS was added as a replacement by volume of fly ash at varying levels of 0, 15, and 30% in the first series, while UFS was used in addition to fly ash by percentage weight of fly ash at the levels of 0, 15, and 30% in the second series. The compressive strength, water absorption, chloride ion penetration, and carbonation depth of the developed ambient-cured GPC were studied. In addition, creep and drying shrinkage of the specimens were also examined. It was found that the compressive strength increased with the UFS content, while the opposite trend was observed with increasing RCA%. The highest compressive strength obtained with 100% RCA was 40.21 MPa (at 90 days), when 30% UFS was used in addition to fly ash. The addition of UFS not only helped in improving the strength characteristics but also provided an alternative to heat curing, which is a major drawback of GPC. Furthermore, the negative effects of RCA can also be minimised by adding UFS, which can be used as a compensator to RCA to improve the durability characteristics. The experimental results prove that susceptibility to chemical, water and chloride attacks can be mitigated by incorporation of UFS, and durable GPC can be produced by using RCA and UFS.

Keywords: recycled coarse aggregate; geopolymer concrete; durability; carbonation; creep; shrinkage

Citation: Arora, S.; Jangra, P.; Pham, T.M.; Lim, Y.Y. Enhancing the Durability Properties of Sustainable Geopolymer Concrete Using Recycled Coarse Aggregate and Ultrafine Slag at Ambient Curing. *Sustainability* **2022**, *14*, 10948. https://doi.org/10.3390/su141710948

Academic Editors: Md Mizanur Rahman, Md Rajibul Karim and Khoi Nguyen

Received: 29 July 2022
Accepted: 29 August 2022
Published: 2 September 2022

1. Introduction

An enormous amount of demolition waste is produced every year. These wastes are usually dumped in landfill or discarded illegally. In recent years, attempts have been made to replace NA with demolished concrete, in particular, the RCA. Considering the aggregate form, the major proportion of concrete (up to 70%), the potential of partially or fully replacing NA with RCA will not only alleviate the accumulation of demolition waste, but also reduce the consumption of NA.

The utilisation of RCA in concrete has been found to degrade the mechanical and durability characteristics of concrete. Detailed discussions have been made in the past regarding the potential benefits and limitations of utilising RCA as a replacement of NA in concrete [1–3]. Their use leads to a rise in water sorptivity, drying shrinkage, and creep of concrete. On the other hand, the mechanical properties, including the compressive strength, flexural strength, and modulus of elasticity, were found to decrease considerably when RCAs were used in concrete [4,5]. Adhesive mortar is present in RCA, which has been identified to be the primary cause of the increased permeability of the final product [6]. In addition, the processing of RCA leads to the formation of cracks, which further increases the probability of permeation [7].

Concrete developed using RCA has been found to show serious durability concerns [6,8,9]. In comparison with the conventional concrete, the concrete with RCA showed 1.3–2.5 times carbonation depth after a curing period of 6 months [10]. Up to a 60% increase in shrinkage was identified when RCAs were used in concrete to replace NA [9]. It has been suggested by some researchers to limit the content of RCA in concrete to 30% so as to fulfil the absorption capacity requirements (5%) of RCA [4,11]. Properties of GPC with RA were studied by Nazarpour and Jamal [12] and the study concluded that the increase in replacement level of RA deteriorated the mechanical properties. Olorunsogo and Padayachee [13] found a rise of 73.2% in chloride conductivity at the age of 28 days when 100% NA was replaced by RCA. Moreover, with the same water-to-binder ratio, carbonation resistance and chloride ion penetration resistance of recycled aggregate concrete (RAC) was found to be lower in comparison with the conventional concrete [6].

From the literature, it can be observed that RCA in concrete adversely affects the mechanical properties of concrete. Meanwhile, to compensate for the negative effects of RCA, geopolymer technology is identified as a potential solution [14,15]. Saravanakumar [15] used fly ash in his investigation based on RAC to enhance RAC properties, and fly ash particles help in compensating for the weaker zone offer by RA by reducing the porosity of the weaker interfacial transition zone (ITZ) and help form an improved matrix. Since RCA offer an alternative to NA and are beneficial from both environmental and economic perspectives, the possibility of their use in concrete with minimal negative effect on its properties deserves the utmost attention. Geopolymer technology utilises pozzolanic materials such as fly ash, slag, and silica fume in place of cement as a binder to produce geopolymer concrete.

The properties of GPC have been observed to be superior in comparison with the conventional concrete [16–18]. Ariffin et al. [19] compared the performance of GPC to conventional concrete under sulphuric acid exposure, and the results indicated an improved performance of GPC. Pozzolanic materials, including fly ash and ground granulated blast furnace slag (GGBS), have been previously utilised by Hwang et al. [20] to enhance the durability properties of concrete developed using RCA. The mechanical properties of fly ash based GPC containing RCA were studied by Nuaklong et al. [21], and the results revealed that the compressive strength of such GPC was found to be at 76–93% of GPC, which contains limestone. Only a slight decrease in the strength and durability characteristics was observed. Concrete mixes of acceptable mechanical properties have been produced when using up to 20% replacement level of NA with RCA, as reported by Marie and Quiasrawi [22]. Durability characteristics of concrete containing RCA were also studied by Kou and Poon [23], in which fly ash was utilised to enhance the properties of RAC.

On the other hand, it was observed by several researchers [24,25] that the properties of GPC considerably improved when slag was added in as a partial replacement of fly ash or in addition to fly ash. Ann et al. [26] investigated the durability properties of RAC and found that fly ash and GGBS compensated the negative effects of RCA. The sulphate resistance of geopolymer RAC was studied by Xie et al. [27], and lower mass loss was observed for RAC containing high content of GGBS. Irrespective of the improved properties of GPC, heat curing condition is a major limitation of the use of GPC. Usually, heat curing is adopted for GPC as it leads to enhanced strength in early stages in comparison with the ambient cured GPC [28]. However, the heat curing requirement of GPC limits its applicability to only the precast industry [17].

In addition to better mechanical performance, concrete structures should have reasonable resistance to environmental impacts. A thorough investigation of chloride ion penetration and carbonation resistance of GPC produced using RCA has not been reported in the literature. Chloride ions are the main cause of corrosion and are responsible for 40% of failure of concrete structures [29]. In marine environment, where chloride ions are present in high concentrations, structural failure mainly occurs due to intrusion of the chloride ions into the concrete. Moreover, no study has focused on the long-term performance of the GPC developed using RCA and UFS. From the perspective of sustainable development, it is crucial to avoid the over utilisation of NA by increasing the use of RCA. Furthermore, it can help in solving the environmental and economic problems associated with the over exploitation of natural resources. This study aimed to develop a sustainable GPC using RCA and UFS with acceptable mechanical and durability properties for structural applications.

Referring to previous studies related to the investigation of RCA properties [14,15], the percentage of RCA varied from 0, 25, 50, to 100%. These replacement levels have been selected so that the maximum percentage of RCA can be utilised. Furthermore, the long-term properties of GPC with RCA were studied in order to understand its potential structural applications with respect to strength and durability aspects. Two series of concrete mixes were produced. For Series I, UFS was used as a replacement by volume of fly ash at various replacement levels (0, 15, and 30%), while it was used as an additive in mixes of Series II as 0, 15, and 30% by weight of fly ash. These two series were chosen to evaluate the feasibility of utilising UFS as a replacement material and as an additive to enhance the durability characteristics of GPC with RCA. Meanwhile, an attempt was made in this study to counteract the main shortcoming of GPC, i.e., heat curing, by using UFS. GPC samples were prepared and examined for compressive strength, water absorption test, chloride ion penetration resistance, carbonation resistance, creep and drying shrinkage. The results of the two series were analysed and compared to understand the effects of UFS on the strength and durability characteristics of RCA. It is anticipated that the addition of UFS enhances the durability characteristics and neutralises the negative effects of RCA in GPC.

2. Testing Program

2.1. Materials

In this investigation, low calcium fly ash conforming to IS 3813 [30] was used as the main binder along with the alkaline solution. UFS was used as a replacement or an additive to fly ash to produce GPC. The chemical composition and physical properties of processed fly ash and UFS are tabulated in Tables 1 and 2, respectively. The density of UFS (850 kg/m^3) was lower than the fly ash (1260 kg/m^3 approximately). Crushed granite and river sand obtained from Yamuna river, India, were used as NA. RCA were procured from a recycling plant in New Delhi, India, and were obtained after recycling the waste from demolished structures based on conventional concrete. NA with three different nominal sizes (7, 10 and 14 mm) and RCA were used. Sieve analysis was conducted in accordance with ASTM C136 [31] to determine the grading of various ingredients.

Table 1. Chemical composition and physical properties of processed fly ash.

Sample	SiO_2 [%]	Al_2O_3 [%]	Fe_2O_3 [%]	SO_3 [%]	CaO [%]	Na_2O [%]	LOI [%]	Specific Surface Area [m^2/kg]
Fly ash	61.17	28.96	3.92	0.25	4.57	0.31	0.66	385
Requirement as per IS:3812 -2003		70% min. by mass		3% max by mass	-	1.5% max by mass	5	320

Figure 1 presents the particle size distribution (PSD) curve of fly ash and UFS, while Figure 2 shows the PSD curve of NA and RCA. Table 3 shows the properties of NA and RCA. It can be seen from Table 3 that the water absorption of RCA was higher (4.25, 4.25, 4.15% for nominal sizes of 7, 10, and 14 mm) in comparison with the water absorption of NA (1.11, 1.12 and 1.18% for the corresponding nominal sizes). Fly ash and UFS were also examined using X-ray diffraction (XRD) to study their microstructure, and the results are depicted in Figure 3. The XRD study shows the presence of high quartz peaks, mullite, calcite, in fly ash, while the UFS indicates an amorphous structure along with calcite compounds. UFS addition results in the formation of improved calcium silicate hydrate (CSH) gel, which fills the voids and leads to a denser structure [32].

Table 2. Chemical composition and physical properties of UFS.

Chemical Composition		Physical Properties	
Constituents	Composition [%]	Physical Property	Results
		Particle Size Distribution [µm]	
SiO_2	35.3	d10	1.8
MgO	6.2	d50	4.4
Al_2O_3	21.4	d90	8.9
Fe_2O_3	1.2	Bulk Density [kg/m^3]	680
SO_3	0.13	Specific Gravity	2.7
CaO	32.2	Specific surface area [m^2/kg]	1200

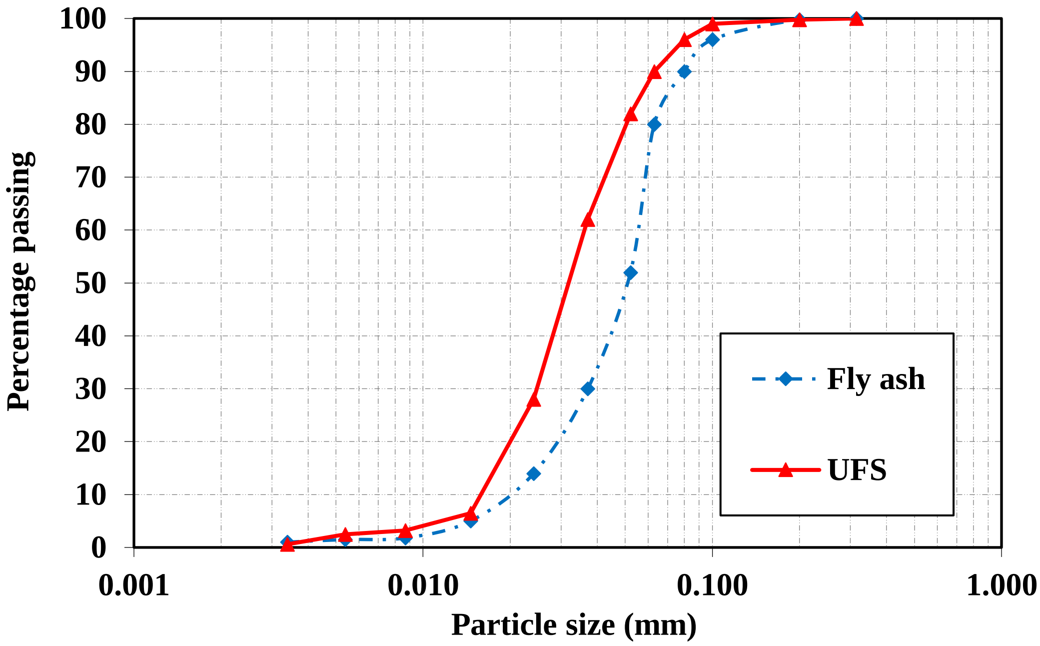

Figure 1. PSD curve of fly ash and UFS.

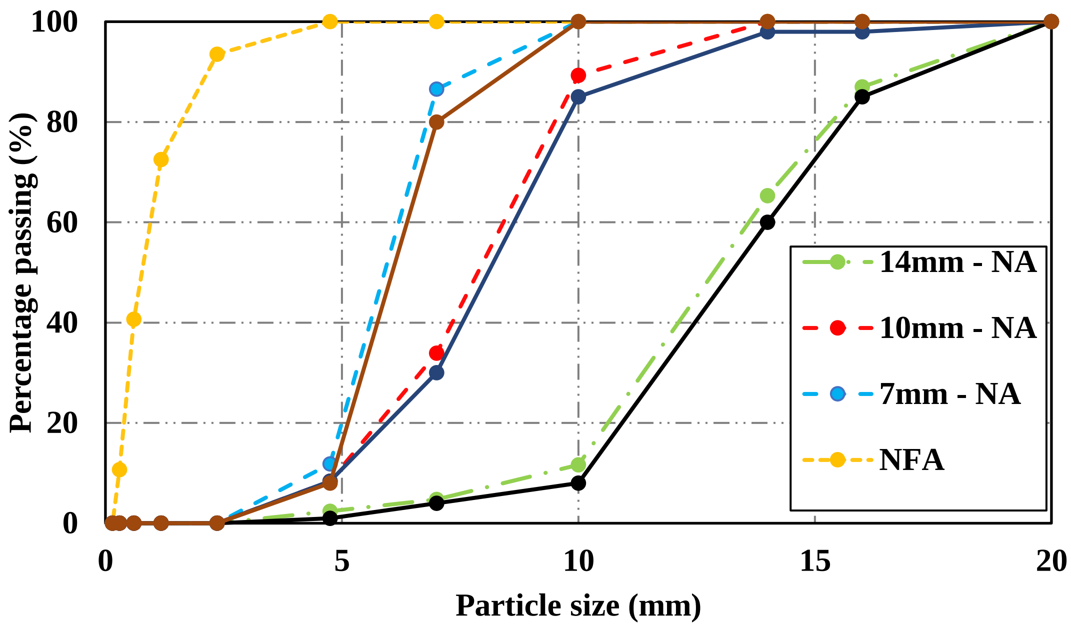

Figure 2. PSD curve of NA and RCA.

Table 3. Properties of NA and RCA.

	Nominal Size (mm)	Density (kg/m^3)	Water Absorption (%)	MIP Porosity (%)
Natural aggregate (NA)	7	2.61	1.11	1.62
	10	2.61	1.12	
	14	2.62	1.18	
Recycle concrete aggregate (RCA)	7	2.46	4.25	8.65
	10	2.58	4.25	
	14	2.58	4.15	

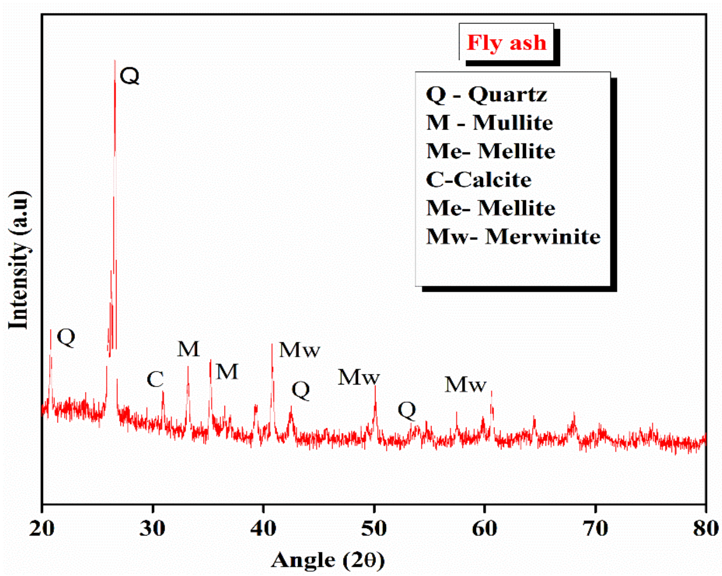

(**a**) XRD of fly ash.

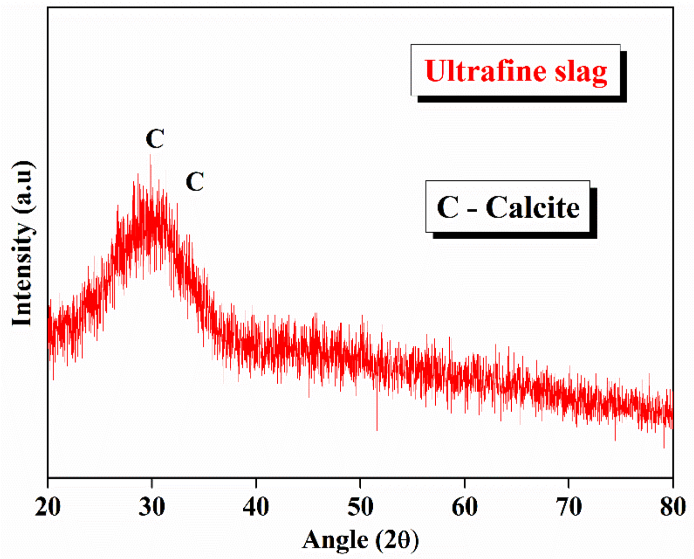

(**b**) XRD of UFS.

Figure 3. XRD of fly ash and UFS.

2.2. Preparation of Specimens

8 M NaOH solution was prepared and allowed to cool for a period of 2–3 h. Then, NaOH solution was mixed with Na_2SiO_3 for 5–7 min to prepare an activator solution,

which was kept at room temperature until final mixing. The solution was prepared 24 h before the final mixing of all the ingredients in the pan mixture. Mix design method developed by Parveen et al. [33] was used to prepare the reference mix for GPC. NA were replaced by RCA in varying proportions of 0, 25, 50, and 100%. The 75% proportions were not considered since it was expected from the outcomes of available literature that only minor variations are generally observed when RCAs with 75 and 100% were replaced.

Two series were classified in accordance with the utilisation of UFS as a replacement to fly ash or an additive to GPC. A total of twelve mixes were prepared in each series, which consisted of 0, 15, and 30% of UFS, and the replacement was conducted by volume of fly ash for mixes of Series I, while the addition of UFS was performed by weight of fly ash for mixes of Series II. These different levels of replacement have been chosen to examine the effects of UFS on the mechanical properties of sustainable GPC. First, four mixes in each series were prepared without UFS and used as a reference for comparison, while the RCA content was varied (0, 25, 50 and 100%) in both series.

Detailed compositions of all the mixes, in kilograms per cubic meter, are presented in Tables 4 and 5, for Series I and Series II, respectively. The concrete mixtures were designated as r-RpSq (where r—replacement; *p* = RCA%; q = UFS%) and a-RpFq (where a—in addition). Various ingredients were initially dry mixed in the pan mixer for three minutes. At the end of the dry mixing process, the activator solution was added, and mixing continued for another four minutes. The specimens were cast and then cured at ambient condition.

Table 4. Mix proportions of GPC mixes Series I (kg/m^3).

Notation	UFS (%)	RCA (%)	Total Liquid				Total Binder Material		Sand	Granite	RCA
			NaOH	Na_2SiO_3	Extra Water	Super plasticiser	FA	UFS			
R0	0	0	48.2	120.5	28	7.5	413	0	521	1215.0	0
R25	0	25	48.2	120.5	28	7.5	413	0	521	911.3	303.8
R50	0	50	48.2	120.5	28	7.5	413	0	521	607.5	607.5
R100	0	100	48.2	120.5	28	7.5	413	0	521	0.0	1215.0
r-R0S15	15	0	48.2	120.5	28	7.5	351.05	61.95	521	1215.0	0
r-R25S15	15	25	48.2	120.5	28	7.5	351.05	61.95	521	911.3	303.8
r-R50S15	15	50	48.2	120.5	28	7.5	351.05	61.95	521	607.5	607.5
r-R100S15	15	100	48.2	120.5	28	7.5	351.05	61.95	521	0.0	1215.0
r-R0S30	30	0	48.2	120.5	28	7.5	289.1	123.9	521	1215.0	0
r-R25S30	30	25	48.2	120.5	28	7.5	289.1	123.9	521	911.3	303.8
r-R50S30	30	50	48.2	120.5	28	7.5	289.1	123.9	521	607.5	607.5
r-R100S30	30	100	48.2	120.5	28	7.5	289.1	123.9	521	0.0	1215.0

Table 5. Mix proportions of GPC mixes Series II (kg/m^3).

Notation	UFS (%)	RCA (%)	Total Liquid				Total Binder Material		Sand	Granite	RCA
			NaOH	Na_2SiO_3	Extra Water	Super plasticiser	FA	UFS			
R0	0	0	48.2	120.5	28	7.5	413	0	521	1215.0	0
R25	0	25	48.2	120.5	28	7.5	413	0	521	911.3	303.8
R50	0	50	48.2	120.5	28	7.5	413	0	521	607.5	607.5
R100	0	100	48.2	120.5	28	7.5	413	0	521	0.0	1215.0
a-R0S15	15	0	48.2	120.5	28	7.5	413	61.95	443	1215.0	0
a-R25S15	15	20	48.2	120.5	28	7.5	413	61.95	443	911.3	303.8
a-R50S15	15	50	48.2	120.5	28	7.5	413	61.95	443	607.5	607.5
a-R100S15	15	100	48.2	120.5	28	7.5	413	61.95	443	0.0	1215.0

Table 5. *Cont.*

Notation	UFS (%)	RCA (%)	Total Liquid				Total Binder Material		Sand	Granite	RCA
a-R0S30	30	0	48.2	120.5	28	7.5	413	123.9	376	1215.0	0
a-R25S30	30	20	48.2	120.5	28	7.5	413	123.9	376	911.3	303.8
a-R50S30	30	50	48.2	120.5	28	7.5	413	123.9	376	607.5	607.5
a-R100S30	30	100	48.2	120.5	28	7.5	413	123.9	376	0.0	1215.0

2.3. Testing of Specimens

In order to obtain the compressive strength of various GPC specimens, axial compression tests were carried out in accordance with the provisions of ASTM C39 [34]. The final compressive strength is the average strength obtained by testing three identical cylindrical specimens, each measuring 150 × 300 mm. For the determination of the water absorption of concrete specimens, water absorption tests were conducted with ASTM C642-13 [35]. The rapid chloride penetration test (RCPT) was conducted as per ASTM C1202 [36] to determine the resistance of concrete to chloride ion penetration. Initially, vacuum saturation was performed, and then the specimens were placed in RCPT migration cells. Three percent NaCl solution and 0.3 M NaOH solution were used as catholyte and anolyte, respectively.

Carbonation depth, which is an indicator of concrete pH was also conducted. Atmospheric carbon dioxide (CO_2) reacts with the calcium hydroxide in cement paste and forms calcium carbonate ($CaCO_3$). Test specimens (100 mm × 100 mm × 400 mm in size) were stored in a chamber, which simulated a controlled environmental condition in accordance with fib CRB-FIP [37]. To determine the creep of various concrete specimens (150 × 300 mm cylinders), the guidelines of ASTM C512/C512M-10 [38] were adopted. The provisions of ASTM C426-16 [39] were used to estimate the drying shrinkage of concrete specimens. All the tests as per their specifications are summarised in Table 6.

Table 6. Experimental tests and relevant standards used to determine concrete properties.

Target Properties	Tests	Standards
Compressive strength	Standard Test method for Compressive Strength of Cylindrical Concrete Specimens	ASTMC39/C39M-20 [34]
Water absorption	Standard test method for density, absorption, and voids in hardened concrete	ASTMC642-13 [35]
Chloride ion penetration	Standard Test Method for Electrical Indication of Concrete's Ability to Resist Chloride Ion Penetration	ASTM C1202- 2012 [36]
Creep	Standard Test Method for Creep of Concrete in Compression	ASTM C512/C512M-10 [38]
Drying shrinkage	Standard Test Method for Linear Drying Shrinkage of Concrete Masonry Units	ASTM C426-16 [39]

3. Results and Discussions

3.1. Compressive Strength

The compressive strength of different GPC mixes was determined at the curing ages of 7, 28, 56 and 90 days. The results of the compressive strength test for Series I and Series II are presented in Tables 7 and 8, respectively. When UFS was not added into GPC, and only fly ash was utilised as a binder material, the 28-day compressive strengths of the mixes R0, R25, R50, and R100 were 22.6, 18.4, 15.2 and 13.8 MPa, respectively. For Series I, when UFS was used to replace 15% of fly ash, the compressive strength ranged between 28 and 38 MPa. Accordingly, when UFS % increased to 30%, the compressive strength also increased with the maximum strength reaching 49.5 MPa for mix r-R0S30, while the minimum strength was 31.4 MPa for mix r-R100S30 (100% RCA). The compressive strength increase was in the range of 34–43% when UFS% was increased from 15 to 30%.

Table 7. Compressive strength (MPa) of Series I GPC mixes.

Notation	7 Days	28 Days	56 Days	90 Days
R0	8.62	22.69	23.82	24.09
R25	7.19	18.43	19.54	20.16
R50	5.96	15.27	15.58	16.53
R100	5.14	13.89	14.03	14.70
r-R0S15	14.75	36.88	37.62	39.54
r-R25S15	12.98	33.27	34.93	37.06
r-R50S15	10.43	27.46	29.11	29.78
r-R100S15	8.19	22.13	23.46	23.72
r-R0S30	19.81	49.52	50.02	51.27
r-R25S30	17.18	44.05	45.37	47.69
r-R50S30	14.67	38.61	40.93	43.50
r-R100S30	11.65	31.49	32.75	34.75

Table 8. Compressive strength (MPa) of Series II GPC mixes.

Notation	7 Days	28 Days	56 Days	90 Days
R0	8.62	22.69	23.82	24.09
R25	7.19	18.43	19.54	20.16
R50	5.96	15.27	15.58	16.53
R100	5.14	13.89	14.03	14.70
a-R0S15	22.78	56.95	59.02	61.01
a-R25S15	19.93	49.34	53.99	55.32
a-R50S15	16.73	43.63	47.07	50.47
a-R100S15	13.05	34.95	37.66	39.61
a-R0S30	23.05	58.03	60.08	62.10
a-R25S30	20.25	50.22	54.91	56.26
a-R50S30	17.04	44.37	47.82	51.27
a-R100S30	13.19	35.51	38.23	40.21

For Series II, when UFS was added into GPC by percentage weight of fly ash, significantly higher strength was observed when compared with Series I. For mixes a-R0S15, a-R25S15, a-R50S15, and a-R100S15, the compressive strength varied in the range of 37–60 MPa. With a further increase in UFS%, an enhancement in the compressive strength was observed, ranging from 38 to 61 MPa.

The compressive strength increase (%) is defined as the ratio of compressive strength of the concrete with varying % of UFS and RCA content to the 28 days compressive strength of the control mix, R0. The compressive strength increases with respect to curing ages are displayed in Figures 4–6. It can be seen from Figures 4–6 that the compressive strength of the GPC significantly increased with increasing UFS content and curing ages. The addition of UFS in the production of GPC filled the pores, as also observed in the previous study [16]. In the study by Parveen et al. [16], UFS was used as an admixture to enhance the properties of fly-ash-based GPC and it helped in filling voids and creating a compact matrix. UFS improved the microstructure by improving interfacial bonding between the paste and the RCA. Furthermore, in Series II, the UFS was added on top of fly ash, which led to denser microstructure. Thus, Series II showed better performance in terms of compressive strength when compared to Series I.

Other potential benefits of UFS are the presence of CaO (32.2%), which helps in the formation of additional calcium products [17]. These calcium products not only provide better bonding, they also accelerate the polymerisation process, which increase the compressive strength. The microstructure of GPC is modified due to the production of additional CSH and CASH gel, which act as micro-aggregate. The additional calcium products formed at the interface of adhered, and new mortar led to an increase in the compressive strength. A decrease in overall void volume led to the formation of a denser and more homogeneous matrix.

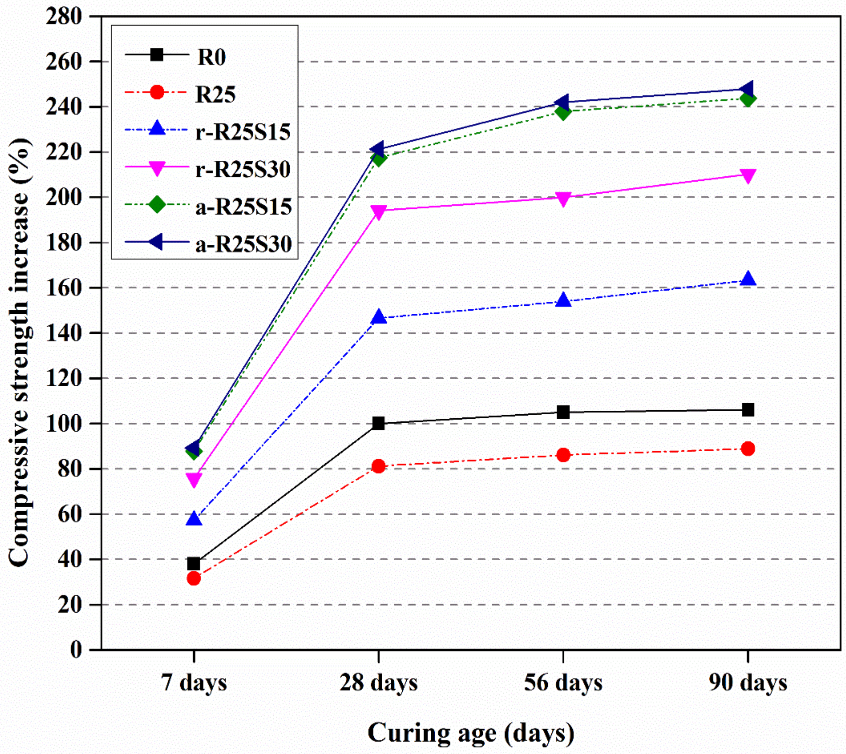

Figure 4. Compressive strength increase of GPC mixes with 25% RCA and varying % of UFS.

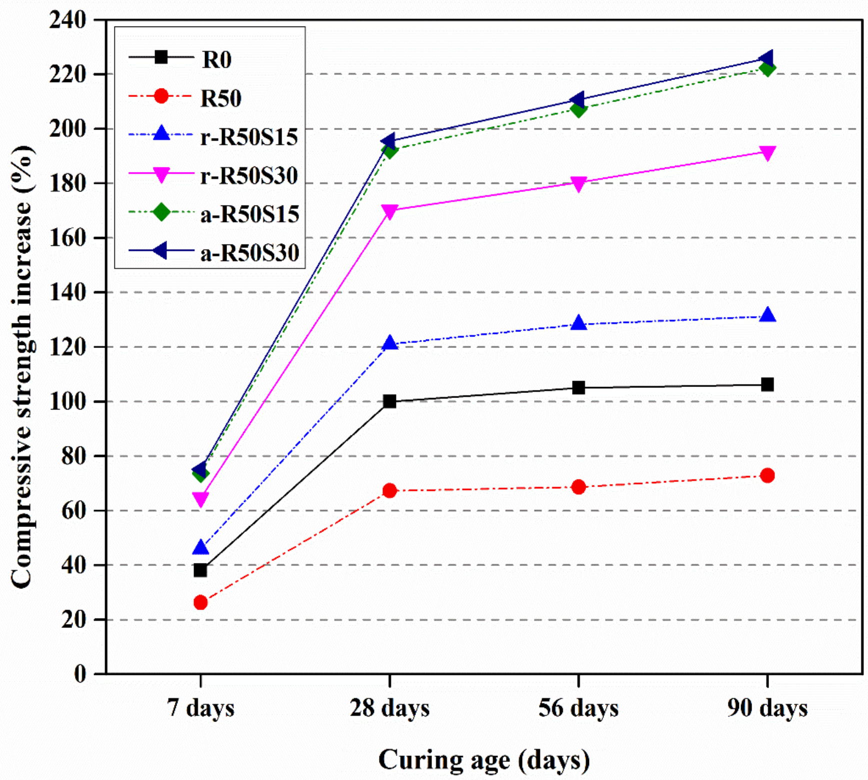

Figure 5. Compressive strength increase of GPC mixes with 50% RCA and varying % of UFS.

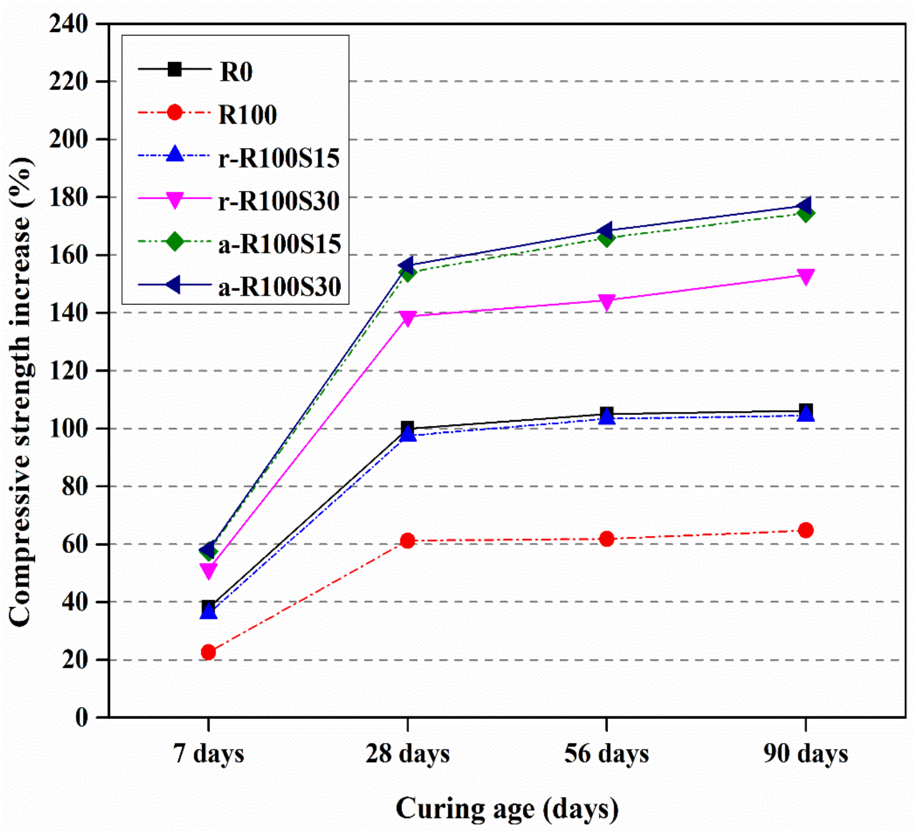

Figure 6. Compressive strength increase of GPC mixes with 100% RCA and varying % of UFS.

Furthermore, with an increase in curing age, the compressive strength also increased, which was similar for all the mixes. Like OPC concrete, the maximum gain in compressive strength was achieved at the age of 28 days, and after that, the strength increase was minimal. Therefore, it can be concluded that GPC produced using RCA and UFS showed similar footprints (in terms of the compressive strength) to that of OPC concrete. A significant increase in the compressive strength was observed when low calcium fly-ash-based GPC was developed incorporating 10% UFS by Saloni et al. [17]. Moreover, the compressive strength gain was highest at the initial stage when UFS was added to produce rice-husk-ash-based GPC [18].

From the Tables 7 and 8, it can be observed that the compressive strength of GPC mixes decreased with an increment in RCA% in GPC, and the trend was similar for all curing ages. The reason behind the decrease in the compressive strength can be attributed to the inferior properties of the RCA in comparison with the NA. Water absorption of RCA (average 4.21%) was higher than water absorption of NA (average 1.13%). Moreover, the mercury intrusion porosimetry (MIP) porosity of RCA was higher (8.65%) than that of NA (1.62%). RCA's higher MIP porosity indicates a porous nature of the RCA, which absorb more water and causing a decrease in the compressive strength. Similarly, high water absorption and MIP porosity create more air voids and hence less dense microstructures. The most significant factor affecting the strength of GPC was its weak ITZ due to RCA incorporation (interface between old mortar and new matrix), which acted as a weak point of failure as a relatively stronger ITZ was formed with NA. This phenomenon was also noticed in previous studies [40]. The mechanical and durability properties of GPC developed using RCA were studied by Shaikh [14], and a declining trend in the compressive strength curve was noticed with an increment in RCA% in GPC. Nuaklong et al. [21] investigated the compressive strength of fly-ash-based GPC containing RA, and the results of the study indicated that compressive strength decreased with an increase in RA%. The outcomes of the above-mentioned studies are well in agreement with the results of the current investigation.

3.2. Water Absorption

The results of the water absorption tests on various GPC mixes of Series I and II are illustrated in Figures 7 and 8, respectively. It can be observed that the water absorption of GPC mixes increased with the RCA%. The water absorption for the reference mixes R0, R25, R50, and R100 at the age of 28 days were 6.7, 9.3, 12.7, and 13.6%, respectively. For Series I, the water absorption at 28 days varied between 5.3 and 10.9% for the mixes r-R0S15, r-R25S15, r-R50S15, and r-R100S15, respectively. However, when UFS content increased from 15 to 30%, the mixes showed a lower water absorption.

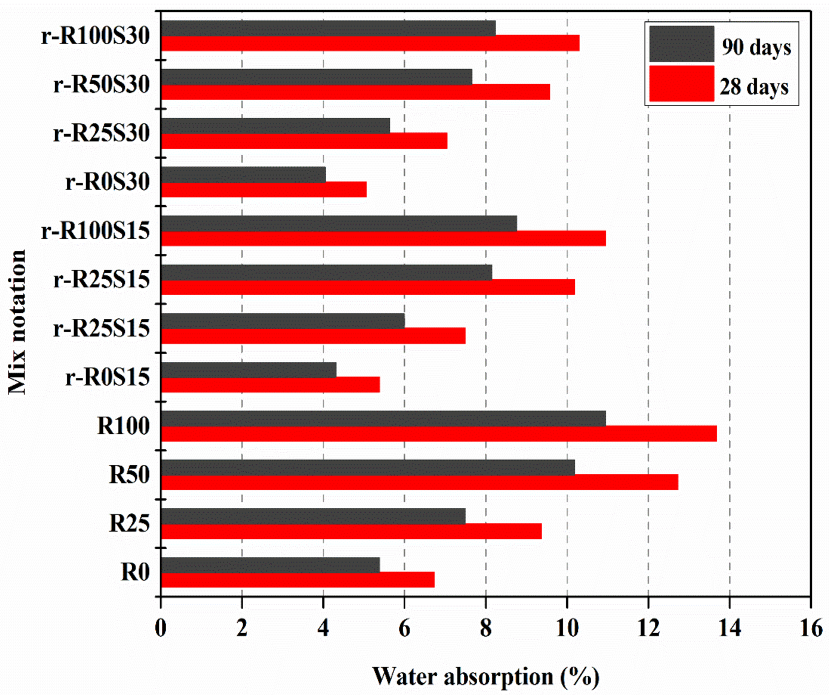

Figure 7. Water absorption of GPC mixes of Series I.

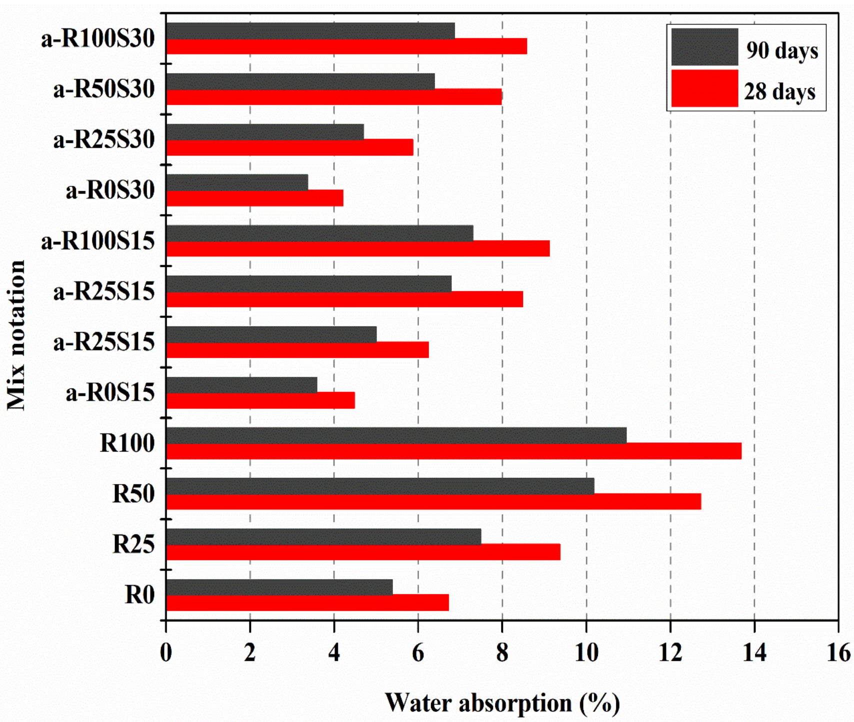

Figure 8. Water absorption of GPC mixes of Series II.

This effect was more significant for Series II where UFS was added on top of fly ash, and lower water absorption was observed in comparison with Series I. Moreover, similar to Series I, the water absorption reduced when UFS addition increased from 15% to 30%. Maximum water absorption (13.6%) was observed for the mix R100. In addition, the water absorption at 90 days was lower in comparison with water absorption at 28 days. Overall, the water absorption increased with the increase in RCA%, and decreased with the increase in UFS content.

The primary cause for increase in water absorption due to the presence of RCA or the increase in RCA% is the higher water absorption of RCA (average 4.21%) than NA (average 1.13%). RCAs are porous in nature due to the presence of mortar, which led to higher water absorption. The mortar attached on the RCA surface had higher porosity, which provided a potential path for water transport in GPC. Shaikh [14] also concluded that the water absorption of RCA-based GPC was high, while investigating the durability properties of GPC using RCA. It is impractical, if not impossible, to thoroughly clean the RCAs before reusing them. Therefore, the presence of residual mortar is unavoidable, which contains more voids leading to increased water absorption. This issue is alleviated with the use of UFS, as the spherical and smaller particles of UFS filled the voids and improved the water absorption capacity. Reduction in water absorption was noticed with increased UFS content. This is beneficial to the durability of GPC. Properties of fly ash GPC were studied by Parveen et al. [16], and it was observed that UFS addition led to a decrease in water absorption of the GPC mixes. Their investigation supported the outcomes of the present study.

3.3. Chloride Ion Penetration

To measure the chloride penetration resistance of the GPC mixes, an RCPT test was carried out, and the results of the RCPT test for Series I and Series II are shown in Figures 9 and 10, respectively. At 28 days, the charges passed in Coulombs for the reference mixes R0, R25, R50, and R100 were observed to be 6132, 6370, 6490, and 6860 Coulombs. This decreased at the age of 90 days, found to be 4856, 4980, 5210 and 5663 Coulombs. Addition of UFS was expected to enhance the microstructure of the GPC with RCA; therefore, RCPT of mixes with UFS in both the series were less than that of the reference mixes. For example, RCPT of mixes r-R0S15, r-R25S15, r-R50S15, and r-R100S15 were found to be 3679, 3822, 3894, and 4116 Coulombs, respectively, while mixes a-R0S30, a-R25S30, a-R50S30 and a-R100S30 showed 2821, 2930, 2985, and 3156 Coulombs, respectively.

Similar to the compressive strength, mixes of Series II showed higher values of RCPT in comparison with the mixes of Series I. The reason for this is obviously the higher UFS content of Series II. Accordingly, it can be concluded that with an increase in RCA%, the RCPT increased for all the mixes, which indicates a poorer resistance of GPC against chloride penetration. Fortunately, this adverse effect can be controlled by adding UFS. For all cases at the age of 90 days, lower RCPT were observed for both the Series in comparison with values obtained at 28 days, which indicates that resistance to chloride ion penetration improves with age. The reduced resistance to chloride penetration with increment in RCA% can again be attributed to the inferior properties of RCA compared with the NA. A new ITZ might have formed at the interface of RCA and new mortar, creating a path for the chloride ions to penetrate into the concrete. The reasons discussed in the section related to the compressive strength above are also applicable here.

Long-term durability properties of RAC containing fly ash were studied by Poon et al. [41], which revealed that with an increase in RCA%, the resistance of concrete mixes to chloride penetration decreased. In addition, the matrix structure improved with age, which was the reason for the decrease in RCPT with age. An investigation was conducted by Parveen et al. [18] on rice-husk-ash-based GPC by incorporating UFS, and the outcomes showed an enhancement in the resistance against chloride penetration when UFS was added into GPC. The results of the above-discussed studies justify the outcomes of the present investigation.

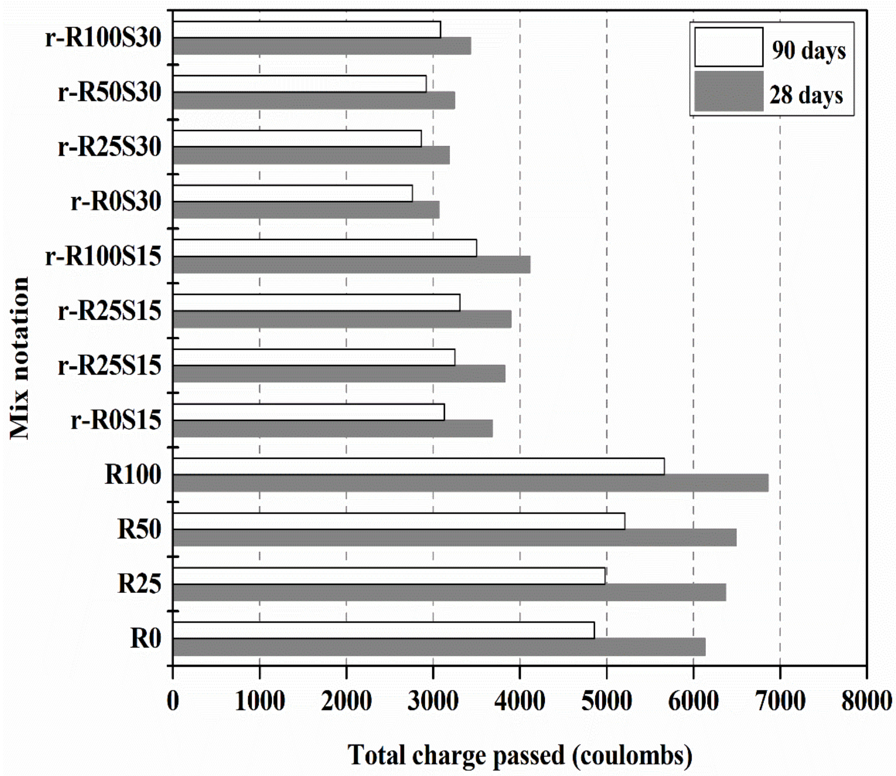

Figure 9. RCPT of GPC mixes of Series I.

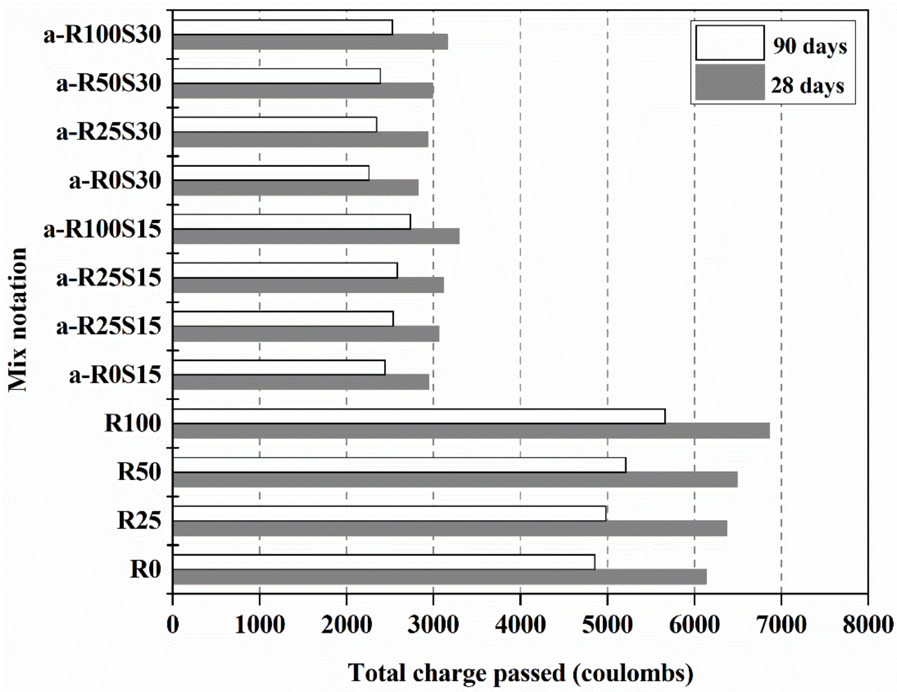

Figure 10. RCPT of GPC mixes of Series II.

3.4. Carbonation Depth

Figures 11 and 12 show the carbonation depth of different GPC mixes of Series I and Series II, respectively. The carbonation depths for the mixes R0, R25, R50, and R100 were 4.1, 6.0, 7.0, and 8.2 mm at 28 days, indicating an increase in carbonation depth with an increase in RCA content. On the other hand, the carbonation depth decreased with the increase in UFS content, which was expected based on the observation from water absorption and chloride penetration. For Series I, the carbonation depths at 28 days were found to be 3.9, 5.5, 6.3, and 7.3 mm for the mixes r-R0S15, r-R25S15, r-R50S15, and r-R100S15, respectively, while for the mixes r-R0S30, r-R25S30, r-R50S30, and r-R100S30, the carbonation depths were observed to be 3.6, 5.2, 5.9, and 6.9 mm, respectively. This decreasing trend of carbonation depth was more pronounced in Series II since its total UFS content of similar mixes was nearly twice that of Series I. The minimum carbonation depth was achieved by mixes a-R0S30, a-R25S30, a-R50S30 and a-R100S30, and the corresponding values were 2.8, 4.0, 4.6, and 5.4 mm, respectively.

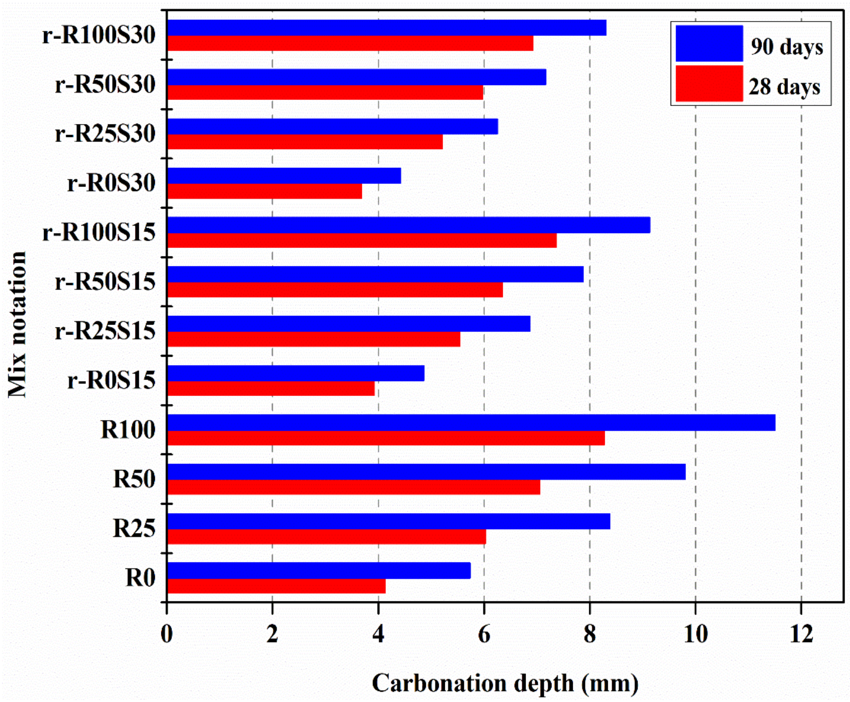

Figure 11. Carbonation depth of GPC of mix Series I.

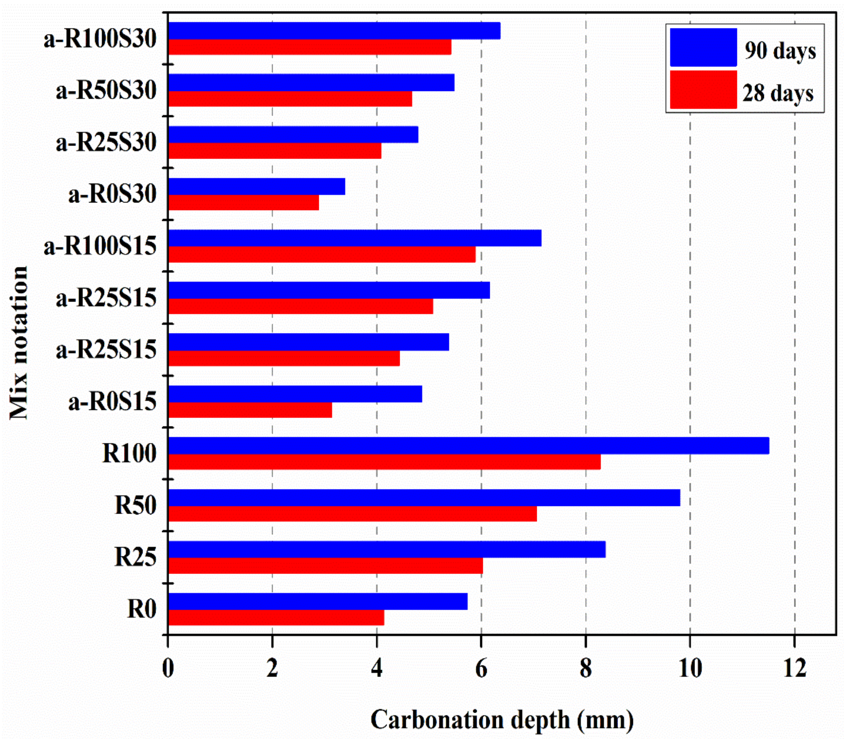

Figure 12. Carbonation depth of GPC of mix Series II.

The same reasons which are responsible for the increase or decrease in water absorption of GPC mixes with the change in RCA% or UFS% are also responsible for the fluctuation in carbonation depth. Carbonation depth of GPC containing RCA was studied by Elchalakani et al. [42] by using fly ash and slag as main binders, and the results showed that carbonation depth increased when RCA% was increased. Parthiban et al. [43] concluded that with the decrease in NA-to-RCA ratio, the carbonation depth increased. The results of the present research agree with the results of their investigation.

3.5. Creep Strain

The creep strain of various GPC mixes was measured at the age of 90 days and are presented in Figure 13. The final creep strain was the average creep strain of three identical specimens. Table 9 shows the percentage change in creep strain of mix Series I and mix Series II with respect to the creep strain of mix R0. It can be seen from Figure 13 that the creep strain increased for both the series with an increase in RCA% in GPC. The minimum value was obtained for the mix R0 (412×10^{-6}), while the maximum value was identified for the mix R100 (502×10^{-6}), out of all the GPC mixes. It indicates that an increase in RCA% leads to higher deformation due to creep. On the other hand, the addition of UFS in GPC was beneficial, as it decreased the creep strain for all the mixes. In general, mixes of Series II showed lower creep than mixes of Series I. The maximum decrease in creep was found to be 25.7% for the mix R0S30.

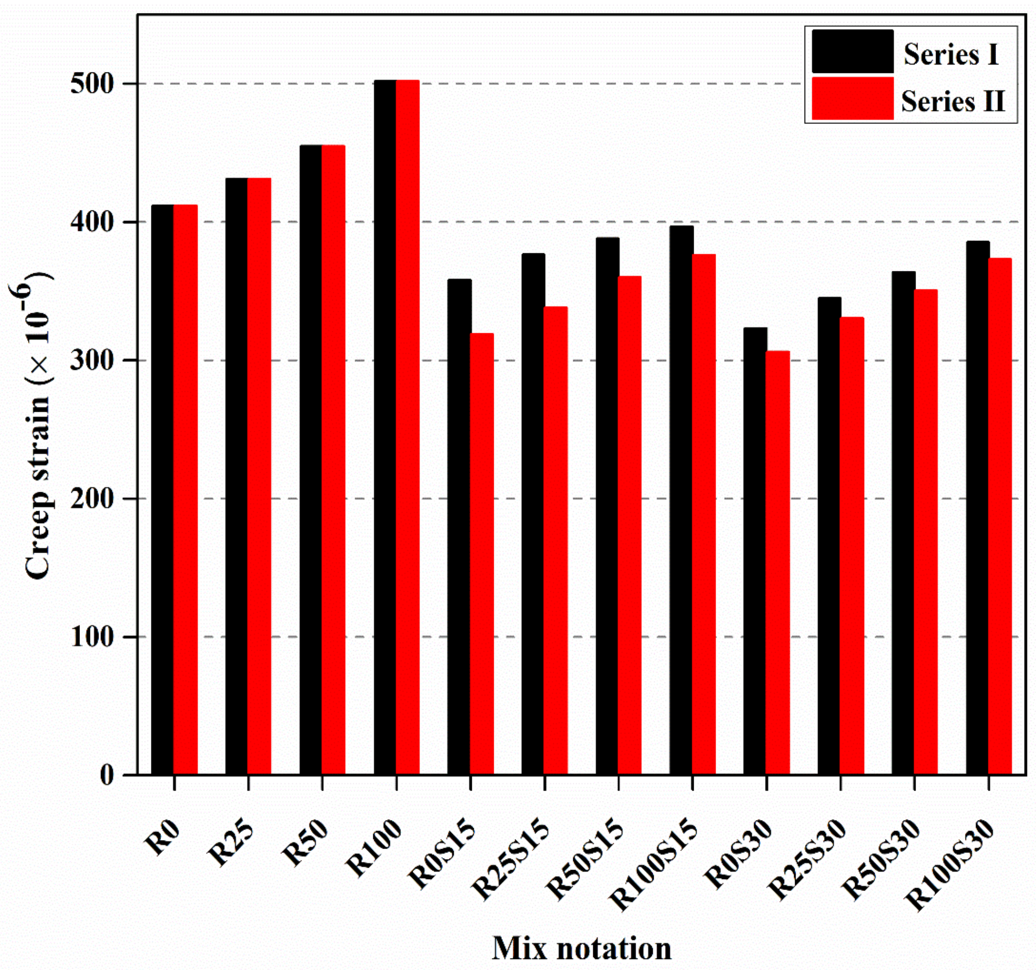

Figure 13. Creep strain of GPC mixes of Series I and Series II at 90 days.

Table 9. Percentage change in creep strain of GPC mixes of Series I and Series II at 90 days.

Notation	% Change in Creep Strain of GPC Mixes at 90 Days in Comparison to Mix R0	
	Series I	Series II
R0	-	-
R25	+(4.7)	-
R50	+(10.4)	-
R100	+(21.8)	-
R0S15	−(13.1)	−(22.6)
R25S15	−(8.6)	−(17.9)
R50S15	−(5.8)	−(12.6)
R100S15	−(3.7)	−(8.7)
R0S30	−(21.5)	−(25.7)
R25S30	−(16.3)	−(19.8)
R50S30	−(11.7)	−(14.9)
R100S30	−(6.4)	−(9.4)

Note that the primary cause of creep increase was the presence of adhesive mortar in recycled aggregate, which resulted in higher total mortar volume, and thus higher creep strain. In contrast, UFS addition improved the matrix structure by filling the voids and reducing the porosity, which lowered the creep strain in GPC. The effect was more pronounced in Series II since the overall UFS content was twice the mixes of Series I. In short, the mixes with the highest amount of UFS (i.e., 30%) showed the best performance in terms of creep strain.

The recorded creep strain for both the series was within the acceptable range for conventional concrete, as mentioned in AS3600 [44]. The relationship between creep strain and aggregate type, air entrainment, and binder loading has been well established, while the relative effect of all these factors on GPC is not certain. In general, in conventional concrete, creep originates due to the formation of a capillary gel containing capillary pores, while in GPC this mechanism is not deeply investigated. Several different mechanisms are responsible for creep, including decomposition and expulsion of the interlayer water, aggregate deformation, which ultimately lead to the formation, or alternatively the breakdown, of the physical bonds.

The creep of concrete containing RCA was investigated by Kou and Poon [23] and the results demonstrated an increase in creep when RCA% was increased in concrete. Effect of UFS addition on properties of metakaolin-based GPC was studied by Parveen et al. [45], and the microstructure was studied by using SEM, EDS and XRD methods, which revealed that UFS enhanced the microstructure of GPC. The studies mentioned above are in support of the experimental outcomes of the present study.

3.6. Drying Shrinkage

Figure 14 displays the drying shrinkage measured at the age of 90 days of GPC mix Series I and mix Series II. Table 10 shows the percentage change in drying shrinkage of various mixes with reference to the drying shrinkage of mix R0. The reported drying shrinkage was also the average values obtained from three identical specimens. From Figure 14, it can be observed that drying shrinkage of GPC mixes increased with an increment in RCA%. The maximum value was obtained for the mix R100 (511×10^{-6}) out of all the GPC mixes. The drying shrinkage for the mixes with UFS were found to be lower in comparison with the mixes without UFS.

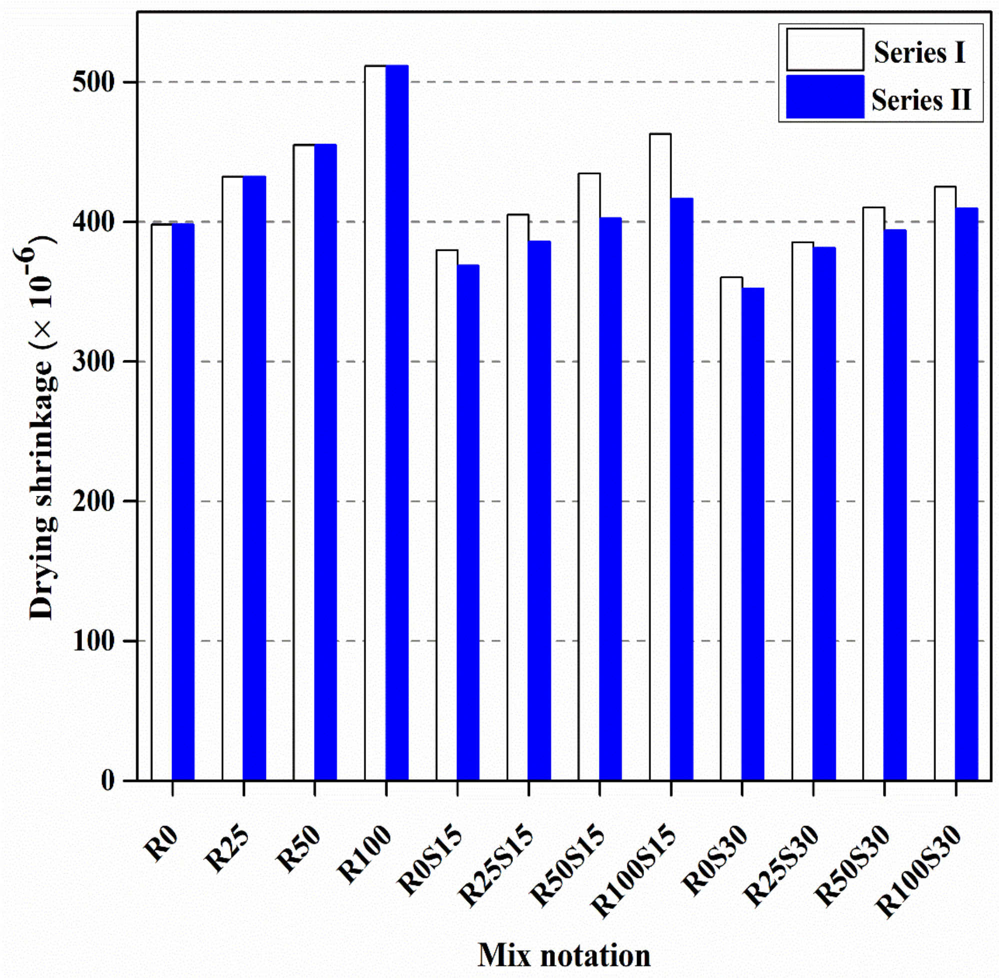

Figure 14. Drying shrinkage of GPC mixes of Series I and Series II at 90 days.

Table 10. Percentage change in drying shrinkage of GPC mixes of Series I and Series II at 90 days.

Notation	% Change in Drying Shrinkage of GPC Mixes at 90 Days in Comparison to Mix R0	
	Series I	Series II
R0	-	-
R25	+(8.6)	-
R50	+(14.3)	-
R100	+(28.5)	-
R0S15	−(4.6)	−(7.4)
R25S15	+(1.8)	−(3.1)
R50S15	+(9.2)	+(1.1)
R100S15	+(16.3)	+(4.7)
R0S30	−(9.5)	−(11.5)
R25S30	−(3.2)	−(4.2)
R50S30	+(3.1)	−(1.1)
R100S30	+(6.8)	+(2.9)

Moreover, the mixes of Series II showed lower drying shrinkage in comparison with mixes of Series I; although, the difference was less significant. The largest increase in drying shrinkage was observed for the mix R100S15 (16.3%) of Series I, while the largest decrease in drying shrinkage was identified as the mix R0S30 (11.5%) of Series II. In this case, pore size distribution (total porosity and average pore diameter) is the critical factor that affects the drying shrinkage of GPC. Large pores were formed due to RCA addition [46], which altered the pore distribution in the matrix and led to higher drying shrinkage. However, UFS acted as a filler primarily and then as an active precursor, which formed the reaction products, such as CSH, CASH and NASH.

Furthermore, the principal mechanism of drying shrinkage was the generation of negative pressure within the capillary network of the concrete. The use of RCA in GPC led to increased mortar volume, which resulted in an increase in drying shrinkage. In contrast, UFS acted as a micro filler as it produced a high quantity of CSH gel, which filled the voids in GPC. This led to the densification of matrix structure, which was the main reason for the lower drying shrinkage of mixes with UFS. UFS addition also led to the formation of a disconnected capillary network, which further reduced the drying shrinkage.

Drying shrinkage of RAC was investigated by Tavakoli and Soroushian [47], and the outcomes of their study indicated an increase in drying shrinkage with an increment in RA% in concrete. A study was conducted by Li and Yao [48] on the drying shrinkage of high-performance concrete containing UFS, and their study mentioned that UFS addition filled the small pores in the concrete and strengthened the structure. The results of the present investigation are justified by the above-discussed studies.

It was found in this study that the addition of RCA adversely affected the durability properties, including water absorption, chloride ion penetration, and carbonation depth of GPC. The adhered mortar with inferior properties created a weak zone between RCA and other GPC ingredients, which contributed to the reduction in strength and degradation in durability characteristics. The adhered mortar also had a higher porosity, which provided a potential route for water transport. The decreased resistance to chloride penetration with an increase in RCA can be due to the inferior properties of RCA relative to NA. The factors affecting the water absorption also affected the carbonation depth of GPC mixes. On an overall scale, creep strain and drying shrinkage of GPC mixes decreased when UFS was included in GPC. It is identified that UFS incorporation in GPC counteracted the harmful effects of RCA addition. Due to UFS addition, the microstructure of GPC was enhanced by the development of additional CSH and CASH gels acting as micro-aggregate. The additional calcium products at the old and the new mortar interface resulted in an improvement in GPC characteristics. Overall, UFS addition enhanced the properties of GPC by acting as a filler and reducing the adverse effects of RCA addition.

4. Conclusions

This study was carried out to examine the durability characteristics of GPC produced using RCA and UFS, in which UFS was used to counteract the negative effects of RCA on GPC characteristics. The following conclusions can be drawn based on the outcomes of the present study:

1. The use of UFS as a partial replacement of or an addition to fly ash enhanced the compressive strength at all replacement levels. The highest percentage increases in compressive strength were 136.3% and 173.5% with 30% UFS and 100% RCA at the age of 90 days, when UFS was used as a partial replacement of fly ash and as an addition to fly ash, respectively.
2. RCA incorporation increased the porosity and thus the water absorption. This was alleviated with the smaller and spherical particle size of UFS, which filled the pores and reduced the water absorption of RCA-based GPC (up to 37.3% decrement).
3. It is a well-known fact that the replacement of NA with RCA increases the chloride ion penetration. This was overcome with the use of UFS, where the resistance of the GPC against chloride ion penetration was reduced.
4. Similar to water absorption, the carbonation depth increased with the increase in RCA content. However, reduced depths were observed for both series of GPC with UFS.
5. The use of UFS as a partial replacement or as an addition to fly ash reduced the creep of the GPC. However, increasing RCA content increased the creep strain of the GPC (412×10^{-6} at 0% RCA to 502×10^{-6} at 100% RCA).

6. GPC with RCA had higher drying shrinkage, and the situation worsened with higher RCA replacement levels. With UFS as a partial replacement or as an addition to fly ash, the drying shrinkage of the GPC was reduced due to the formation of a disconnected capillary network.

Therefore, it can be concluded from the results of this study that UFS can be utilised as a compensator to RCA for enhancing the durability characteristics of GPC. Furthermore, it can be used as a partial replacement of fly ash or as an addition to fly ash in the GPC mix design. Although the use of UFS is sustainable from the economic and environmental point of view, efforts are required to improve the cost-effectiveness of GPC.

Author Contributions: Conceptualization, S.A.; software, S.A., Y.Y.L.; data curation, S.A., P.J.; writing—original draft preparation, S.A., P.J., T.M.P.; methodology, P.J.; visualization, P.J.; investigation, P.J.; supervision, P.J. and Y.Y.L.; funding acquisition, T.M.P.; reviewing and editing, P.J., T.M.P. and Y.Y.L. All authors have read and agreed to the published version of the manuscript.

Funding: This research received no external funding.

Institutional Review Board Statement: Not applicable.

Informed Consent Statement: Not applicable.

Data Availability Statement: Not applicable.

Acknowledgments: The authors wish to thank Raicon Labs Private Limited, Haryana, India, for giving support to test the samples in their laboratory. The financial support from Small Grant, Curtin University, is greatly appreciated.

Conflicts of Interest: The authors declare no conflict of interest.

Abbreviations

CSH	Calcium silicate hydrate gel
CASH	Calcium aluminate silicate hydrate
CO_2	Carbon dioxide
$CaCO_3$	Calcium carbonate
GPC	Geopolymer concrete
GGBS	Ground granulated blast furnace slag
ITZ	Interfacial transition zone
MIP	Mercury intrusion porosimetry
NA	Natural aggregate
SH	Sodium hydroxide
SS	Sodium silicate
PSD	Particle size distribution
RAC	Recycled aggregate concrete
RCA	Recycled coarse aggregate
RCPT	Rapid chloride permeability test
UFS	Ultrafine slag
XRD	X-ray diffraction

References

1. Hansen, T.C. *Recycling of Demolished Concrete and Masonry*; CRC Press: Boca Raton, FL, USA, 2014. [CrossRef]
2. Sagoe-Crentsil, K.K.; Brown, T.; Taylor, A.H. Performance of concrete made with commercially produced coarse recycled concrete aggregate. *Cem. Concr. Res.* **2001**, *31*, 707–712. [CrossRef]
3. Martirena-Hernandez, J.F.; Alujas-Díaz, A.; Amador-Hernandez, M. *Proceedings of the International Conference of Sustainable Production and Use of Cement and Concrete*; Springer: Cham, Switzerland, 2020.
4. Kwan, W.H.; Ramli, M.; Kam, K.J.; Sulieman, M.Z. Influence of the amount of recycled coarse aggregate in concrete design and durability properties. *Constr. Build. Mater.* **2012**, *26*, 565–573. [CrossRef]
5. Dhir, R.K.; Limbachiya, M.C.; Leelawat, T. Suitability of recycled concrete aggregate for use in BS 5328 designated mixes. *Proc. Inst. Civ. Eng. Struct. Build.* **1999**, *134*, 257–274. [CrossRef]

6. Otsuki, N.; Miyazato, S.; Yodsudjai, W. Influence of Recycled Aggregate on Interfacial Transition Zone, Strength, Chloride Penetration and Carbonation of Concrete. *J. Mater. Civ. Eng.* **2003**, *15*, 443–451. [CrossRef]
7. Olorunsogo, F.T.; Padayachee, N. Performance of recycled aggregate concrete monitored by durability indexes. *Cem. Concr. Res.* **2002**, *32*, 179–185. [CrossRef]
8. Evangelista, L.; de Brito, J. Durability performance of concrete made with fine recycled concrete aggregates. *Cem. Concr. Compos.* **2010**, *32*, 9–14. [CrossRef]
9. Hansen, T.C.; Boegh, E. Elasticity and Drying Shrinkage of Recycled-Aggregate Concrete. *J. Am. Concr. Inst.* **1985**, *82*, 648–652. [CrossRef]
10. Levy, S.M.; Helene, P. Durability of recycled aggregates concrete: A safe way to sustainable development. *Cem. Concr. Res.* **2004**, *34*, 1975–1980. [CrossRef]
11. Fomento, M. *Instrucción de Hormigón Estructural (EHE-08)*; Gobierno de España, Ministerio de Fomento: Madrid, Spain, 2008.
12. Nazarpour, H.; Jamali, M. Mechanical and freezing cycles properties of geopolymer concrete with recycled aggregate. *Struct. Concr.* **2020**, *21*, 1004–1012. [CrossRef]
13. Domingo-Cabo, A.; Lázaro, C.; López-Gayarre, F.; Serrano-López, M.A.; Serna, P.; Castaño-Tabares, J.O. Creep and shrinkage of recycled aggregate concrete. *Constr. Build. Mater.* **2009**, *23*, 2545–2553. [CrossRef]
14. Shaikh, F.U.A. Mechanical and durability properties of fly ash geopolymer concrete containing recycled coarse aggregates. *Int. J. Sustain. Built Environ.* **2016**, *5*, 277–287. [CrossRef]
15. Saravanakumar, P. Strength and durability studies on geopolymer recycled aggregate concrete. *Int. J. Eng. Technol.* **2018**, *7*, 370–375. [CrossRef]
16. Parveen; Singhal, D.; Junaid, M.T.; Jindal, B.B.; Mehta, A. Mechanical and microstructural properties of fly ash based geopolymer concrete incorporating alccofine at ambient curing. *Constr. Build. Mater.* **2018**, *180*, 298–307. [CrossRef]
17. Saloni; Singh, A.; Sandhu, V.; Jatin; Parveen. Effects of alccofine and curing conditions on properties of low calcium fly ash-based geopolymer concrete. *Mater. Today Proc.* **2020**, *32*, 620–625. [CrossRef]
18. Parveen; Singhal, D.; Jindal, B.B. Experimental study on geopolymer concrete prepared using high-silica RHA incorporating alccofine. *Adv. Concr. Constr.* **2017**, *5*, 345–358. [CrossRef]
19. Ariffin, M.A.M.; Bhutta, M.A.R.; Hussin, M.W.; Tahir, M.M.; Aziah, N. Sulfuric acid resistance of blended ash geopolymer concrete. *Constr. Build. Mater.* **2013**, *43*, 80–86. [CrossRef]
20. Hwang, J.P.; Shim, H.B.; Lim, S.; Ann, K.Y. Enhancing the durability properties of concrete containing recycled aggregate by the use of pozzolanic materials. *KSCE J. Civ. Eng.* **2013**, *17*, 155–163. [CrossRef]
21. Nuaklong, P.; Sata, V.; Chindaprasirt, P. Influence of recycled aggregate on fly ash geopolymer concrete properties. *J. Clean. Prod.* **2016**, *112*, 2300–2307. [CrossRef]
22. Marie, I.; Quiasrawi, H. Closed-loop recycling of recycled concrete aggregates. *J. Clean. Prod.* **2012**, *37*, 243–248. [CrossRef]
23. Kou, S.C.; Poon, C.S. Enhancing the durability properties of concrete prepared with coarse recycled aggregate. *Constr. Build. Mater.* **2012**, *35*, 69–76. [CrossRef]
24. Nath, P.; Sarker, P.K. Effect of GGBFS on setting, workability and early strength properties of fly ash geopolymer concrete cured in ambient condition. *Constr. Build. Mater.* **2014**, *66*, 163–171. [CrossRef]
25. Jindal, B.B.; Singhal, D.; Sharma, S.K.; Jangra, P. Suitability of Ambient-Cured Alccofine added Low-Calcium Fly Ash-based Geopolymer Concrete. *Indian J. Sci. Technol.* **2017**, *10*, 1–10. [CrossRef]
26. Ann, K.Y.; Moon, H.Y.; Kim, Y.B.; Ryou, J. Durability of recycled aggregate concrete using pozzolanic materials. *Waste Manag.* **2008**, *28*, 993–999. [CrossRef]
27. Xie, J.; Zhao, J.; Wang, J.; Wang, C.; Huang, P.; Fang, C. Sulfate resistance of recycled aggregate concrete with GGBS and fly ash-based geopolymer. *Materials* **2019**, *12*, 1247. [CrossRef] [PubMed]
28. Nurruddin, E.A. Methods of curing geopolymer concrete: A review. *Int. J. Adv. Appl. Sci.* **2018**, *5*, 31–36. [CrossRef]
29. Chloride Attacks on Concrete Structures. Available online: https://www.ctlgroupqatar.com/single-post/2019/02/02/chloride-attacks-on-concrete-structures (accessed on 31 January 2021).
30. *IS: 3812, BIS 3812*; Specification for Pulverized fuel ash, Part-1: For Use as Pozzolana in Cement, Cement Mortar and Concrete. Bureau of Indian Standards: New Delhi, India, 2013.
31. *ASTM C136/C136M-19*; Standard Test Method for Sieve Analysis of Fine and Coarse Aggregates. American Society of Testing and Materials: West Conshohocken, PA, USA, 2014.
32. Reddy, P.N.; Naqash, J.A. Experimental study on TGA, XRD and SEM analysis of concrete with ultra-fine slag. *Int. J. Eng. Trans. B Appl.* **2019**, *32*, 679–684. [CrossRef]
33. Parveen; Singhal, D. Development of mix design method for geopolymer concrete. *Adv. Concr. Constr.* **2017**, *5*, 377–390. [CrossRef]
34. *ASTM C39/C39M-18*; Standard Test Method for Compressive Strength of Cylindrical Concrete Specimens. ASTM International: West Conshohocken, PA, USA, 2020.
35. *ASTM C642-13*; Standard Test Method for Density, Absorption, and Voids in Hardened Concrete. ASTM International: West Conshohocken, PA, USA, 2013.
36. *ASTM C1202*; Standard Test Method for Electrical Indication of Concrete's Ability to Resist Chloride Ion Penetration. American Society of Testing and Materials: West Conshohocken, PA, USA, 2012.

37. FIB-CEB-FIP, Model Code 2010. 2010. Available online: https://www.fib-international.org/publications/model-codes.html (accessed on 28 July 2022).
38. *ASTM C512/C512M-10*; Standard Test Method for Creep of Concrete in Compression. ASTM International: West Conshohocken, PA, USA, 2010.
39. *ASTM C426-16*; Standard Test Method for Linear Drying Shrinkage of Concrete Masonry Units. ASTM International: West Conshohocken, PA, USA, 2016.
40. Wang, H.L.; Wang, J.J.; Sun, X.Y.; Jin, W.L. Improving performance of recycled aggregate concrete with superfine pozzolanic powders. *J. Cent. South Univ.* **2013**, *20*, 3715–3722. [CrossRef]
41. Kou, S.C.; Poon, C.S. Long-term mechanical and durability properties of recycled aggregate concrete prepared with the incorporation of fly ash. *Cem. Concr. Compos.* **2013**, *37*, 12–19. [CrossRef]
42. Elchalakani, M.; Dong, M.; Karrech, A.; Li, G.; Ali, M.S.M.; Xie, T.; Yang, B. Development of Fly Ash- and Slag-Based Geopolymer Concrete with Calcium Carbonate or Microsilica. *J. Mater. Civ. Eng.* **2018**, *30*, 04018325. [CrossRef]
43. Parthiban, K.; Mohan, K.S.R. Influence of recycled concrete aggregates on the engineering and durability properties of alkali activated slag concrete. *Constr. Build. Mater.* **2017**, *133*, 65–72. [CrossRef]
44. *AS 3600-2009*; Concrete Structures. Australian Standards: Sydney, NSW, Australia, 2009.
45. Parveen; Mehta, A.; Saloni. Effect of ultra-fine slag on mechanical and permeability properties of Metakaolin-based sustainable geopolymer concrete. *Adv. Concr. Constr.* **2019**, *7*, 231–239. [CrossRef]
46. Guo, Y.; Qian, J.; Wang, X. Pore structure and influence of recycled aggregate concrete on drying shrinkage. *Math. Probl. Eng.* **2013**, *2013*, 912412. [CrossRef]
47. Tavakoli, M.; Soroushian, P. Drying shrinkage behavior of recycled aggregate concrete. *Am. Concr. Inst.* **1996**, *18*, 58–61.
48. Li, J.; Yao, Y. A study on creep and drying shrinkage of high performance concrete. *Cem. Concr. Res.* **2001**, *31*, 1203–1206. [CrossRef]